



Application of nonlinear regression in recognizing distribution of signals in wireless channels

Dragiša Miljković*, Siniša Ilić, Dragana Radosavljević and Stefan Pitulić

Faculty of Technical Sciences, University of Pristina in Kosovska Mitrovica, Knjaza Milosa 7, 38220 Kosovska Mitrovica, Serbia

Received 11 September 2022, accepted 7 December 2022, available online 16 March 2023

© 2023 Authors. This is an Open Access article distributed under the terms and conditions of the Creative Commons Attribution 4.0 International License CC BY 4.0 (<http://creativecommons.org/licenses/by/4.0>).

Abstract. In many applications, it is important to recognise the distribution of empirical data in almost real time. One of the specific applications is the identification of statistical models for fading in wireless systems of the base station receivers. This is one of the most important problems in spatial diversity. In this paper, we describe the methodology and the results of a nonlinear regression approach for recognising the distribution of the input signal with the values of its parameters. Furthermore, the proposed approach could be used for the real-time recognition of the probability distributions without any prior knowledge about the input signal. To prove its performance, the Levenberg–Marquardt nonlinear least-squares algorithm is tested on a large set of randomly generated signals with the Gamma, Rayleigh, Rician, Nakagami-m, and Weibull distributions. The experimental results demonstrate that this approach is accurate in recognizing statistical distributions from the signal.

Keywords: data mining, classification, nonlinear regression, curve fitting, probability distribution.

1. INTRODUCTION

One of the fundamental challenges in data processing is finding a way to describe the data characteristics, i.e. finding its statistical description. A number of techniques with good predictive capabilities have been developed in the field of machine learning. Regression analysis remains relevant due to its simplicity and flexibility as well as the ease of understanding the processes that take place and interpreting parameters in them. Linear regression models have lower complexity and they are easy to use and interpret. However, they fail to fit complex datasets properly. Nonlinear regression (NR) model fitting and parameter estimation is the best approach for analysing many types of data [1]. The goal of NR is to iteratively find the values of parameters that minimize the sum-of-squares of differences between the estimated and the measured values. It starts with the initial values of

parameters and is followed by adjusting those values, until the best possible fit is found or until the maximum number of iterations is reached.

In general terms, NR can be described by the following formula:

$$y = f(x, \theta) + \varepsilon, \quad (1)$$

where f is the response function, x is the input (n -dimensional vector of predictors), θ is the k -dimensional vector of parameter estimates that is to be calculated, and ε is the error [2].

NR is used in a wide range of scientific and technical fields for the analysis and interpretation of nonlinear fitting to data. The natural nonlinearity of the processes in medicine makes this field suitable for the application of NR, e.g., in the fields of cancer dependencies identification [3], split-belt treadmill walking [4], electromyography techniques for rehabilitation [5], and CT imaging [6]. Other areas for NR application are renewable energy

* Corresponding author, dragisa.miljkovic@pr.ac.rs

technologies and ecology, where NR is useful for predicting the biogas production rate [7], air quality modelling [8], and wastewater treatment [9]. In the previous two years, after the outbreak of the COVID-19 virus pandemic, NR has been used in attempts to describe and understand the impact of risk factors in death rate [10], environmental factors impacting the epidemic [11], or even forecasting a model for predicting COVID-19 infection rates [12]. Furthermore, NR is especially present in the field of computer vision, where it is widely used for counting people at mass gatherings, age assessment, visual tracking, and image super-resolution [13].

One of the main goals in wireless communication systems design is to achieve the desired quality of service and grade of service in terms of the spectral efficiency requirements of the received signal. Among the key issues within this process is the analysis of properties and impacts that any type of interference has on wireless communication. Efficient receiving systems operation is heavily dependent on a reliable assessment of the received signal model and its parameters.

Propagation of the wireless signal through the atmosphere is characterized by temporal fluctuations in the envelope and phase shifts of the transmitted signal. These changes in the level of the useful signal over time are called fading [14]. Fading leads to the reception of signals of poor quality. Several distribution models can be used to describe signal envelope fluctuations in fading channels: Nakagami-m, Weibull, Rayleigh, Nakagami-q (Hoyt), Rician, α - μ , κ - μ , η - μ , α - κ - μ , α - η - μ [14,15].

Various diversity techniques are implemented to reduce the impact of fading and interchannel interference, the most important of which are space, time, and frequency diversity. A diversity receiver listens to signals on multiple antennas in order to accurately estimate a fading channel model and to optimize its parameters [14]. The diversity receiver may estimate features of the signals at their input by determining the signals' distribution types and the parameters of these distributions.

Several approaches have been developed for statistical model recognition using different methods [16]. When it comes to estimating fading channel parameters, there are numerous examples of estimators based on the method of moments [17] and the method of maximum likelihood [18]. Attempts have also been made to deal with this matter by using deep learning [19], however, overall, this remains an open issue for future research and performance improvement.

This paper explores the application of NR algorithms in the assessment and recognition of signal characteristics at the inputs of antennas at the base station receiver with the aim of improving communication system performance. The approach that is used in the paper is concerned with identifying the statistical models of the received signals

and estimating the parameters of the identified statistical distribution. A special advantage of this approach is that no prior knowledge about the signal characteristics is necessary, and signal processing is possible in almost real time.

The remainder of this paper is structured as follows: first, we present an overview of the distribution models we used in signal recognition. Second, we outline the methodology and describe the data used to test the approach. Third, we present the results and discussion, followed by concluding remarks on the performance and possibilities of using this approach.

2. DISTRIBUTION MODELS

A base station receiver needs to make a selection of several received signals and use the one with the best characteristics, which makes it highly important to recognise both the distributions of the signals at the input of a receiver and their parameters. For this paper, we selected some of the most frequent distributions of the signal's envelopes found in the literature for a base station receiver [20]: Gamma, Rayleigh, Rician, Nakagami-m, and Weibull.

The probability density function (PDF) of the **Gamma** model can be described as [14]:

$$f_R(r) = \frac{r^{c-1}}{\Gamma(c)\Omega^c} e^{-\frac{r}{\Omega}}, r > 0, \quad (2)$$

where $\Omega = 2\sigma^2$ is the scale parameter, e.g. the average signal power (defined as $\Omega = E(r^2)$, where E is the mathematical expectation of a statistical process), and c is the shape parameter.

The PDF of the **Rayleigh** model can be described as [21]:

$$f_R(r) = \frac{2r}{\Omega} \exp\left(-\frac{r^2}{\Omega}\right), \quad (3)$$

where Ω is the scale parameter.

The PDF of the **Rician** model is [21]:

$$f_R(r) = \frac{2(1+K)r}{e^{\kappa}\Omega} \exp\left(-\frac{(1+K)r^2}{\Omega}\right) \times I_0\left[2\sqrt{\frac{K(1+K)r^2}{\Omega}}\right], \quad (4)$$

where K is the Rician factor, Ω is the scale parameter, and $I_0[\cdot]$ is the zeroth order modified Bessel function of the first kind. When K increases, the impact of Rician fading is declining and system performance increases. When the Rician factor K increases, then the Rician channel becomes the channel without fading. When the Rician factor K goes to zero, the Rician model becomes the Rayleigh model [22].

The PDF of the **Nakagami-m** model is [23]:

$$f_R(r) = \frac{2m^m r^{2m-1}}{\Gamma(m)\Omega^m} \exp\left(-\frac{mr^2}{\Omega}\right), \quad 0 \leq r < \infty, \quad (5)$$

where $\Gamma[\cdot]$ is the Gamma function, Ω is the scale parameter, and m is the Nakagami fading parameter. When m increases, the sharpness of the fading decreases. When $m = 1$, the Nakagami- m channel becomes the Rayleigh channel. When m goes to infinity, the Nakagami- m model becomes a model without fading [21].

The PDF of the **Weibull** model is [14]:

$$f_R(r) = \frac{\alpha r^{\alpha-1}}{\Omega} \exp\left(-\frac{r^\alpha}{\Omega}\right), \quad (6)$$

where α is the shape parameter and Ω is the scale parameter. When $\alpha = 2$, the Weibull model becomes the Rayleigh model, and when α goes to infinity, the Weibull model becomes a model without fading. The sharpness of the fading depends on the parameter α [24].

3. METHODOLOGY

The probability distribution of the signal and its parameter estimations can be assessed using data analysis methods. Since we could not access the real signal data at the input of the base station receiver, we used randomly generated signals' sample data in line with the most frequent distributions of the signal's envelopes found in literature [20]. Subsequently, we designed and applied the recognition of the signals' data distributions and their parameters in receiver's logic by using NR.

To simulate signal samples at the inputs of a receiver, and to measure model recognition algorithm efficiency, we generated a set of test data that is sufficiently large to evaluate the preciseness of the estimates. We used the MATLAB software (Release 2021a) built-in *makedist* function to generate random sample values for the selected probability distributions and their parameter values.

In the preparation phase, distribution parameter values of the generated signals are chosen to correspond to the cases that may be encountered in reality, in accordance with the reference value ranges given in [25]. In each of the five distributions, the scale parameter Ω varies from 1 to 2.5 in increments of 0.1. Additionally, the following parameter values are used in four distributions:

- Gamma distribution: five values of parameter c , from 1 to 3 in increments of 0.5,
- Nakagami- m distribution: six values of parameter m , starting with 0.5, and from 1 to 5 in increments of 1,
- Rician distribution: six values of parameter K , from 0 to 5, in increments of 1,
- Weibull distribution: six values of parameter c , from 0.5 to 3 in increments of 0.5.

In order to obtain fair results in the evaluation (recognition) of a probability distribution and its parameter values from the test signal samples, 100 signals were generated for each of the 384 different parameter com-

binations. Thus, a total of 38 400 different signals were used in this experiment (one signal consists of N_s randomly generated values).

The process of parameter estimation of a probability distribution is based on finding the model, which best fits the signal data points. Since the regression finds the best parameter values by minimizing the error between the values of real data against the calculated values from mathematical equations (the reference values), we decided to calculate these parameters not directly from the test data signal values, but from their discretised Cumulative Density Functions (dCDF).

In order to better present how the normalised dCDF is calculated from the sample values of the input signal, we generated 20 signal samples that follow a distribution selected in the random generator (in this case – Gamma distribution with parameters $\Omega = 1$ and $c = 2$), which are presented in Fig. 1. As can be seen, the generated sample values in this example are in the range of 0.165–9.475. This value range is then divided into several subranges (bins; see column *Bin MaxV* in Fig. 2). The dCDF value of each bin is calculated as the number of sample values that are less than or equal to its maximum value (i.e. the number of sample values that are less or equal to the maximum value of the fourth bin in this example is 17, as shown in column *dCDF*). At the end of the process, the dCDF is normalised (divided) by the total number of samples (column *normalised dCDF*). By selecting values from columns *Bin MaxV* and *normalised dCDF* for x and y axes, respectively, we prepared the coordinates of data points for curve fitting in the next steps of the NR application.

Signal values: 0.227531, 1.80523, 0.165631, 1.24947, 5.08724, 3.10942, 1.14969, 1.28665, 3.66837, 9.47541, 3.14633, 2.65018, 1.58915, 3.29589, 0.33547, 1.06296, 1.70372, 1.23008, 0.766655, 1.8028

Bin #	Bin MaxV	dCDF	normalized dCDF
1	0	0	0
2	1.15	6	0.3
3	2.3	13	0.65
4	3.45	17	0.85
5	4.6	18	0.9
6	5.75	19	0.95
7	6.9	19	0.95
8	8.05	19	0.95
9	9.2	19	0.95
10	10.35	20	1

$\mathbf{x} = (0, 1.15, 2.3, 3.45, 4.6, 5.75, 6.9, 8.05, 9.2, 10.35)$

$\mathbf{y} = (0, 0.3, 0.65, 0.85, 0.9, 0.95, 0.95, 0.95, 0.95, 1)$

Fig. 1. Calculating normalised dCDF of the signal's sample values.

```

1 Input: input signal, probability distribution models
2 // Preparation phase:
3   Find max sample value
4    $bean\_size = max\_sample / number\_of\_beans$ 
5   for  $i \leftarrow 1, number\_of\_beans$  do
6      $beans[i] = i * bean\_size$ 
7   end for
8   for  $i \leftarrow 1, number\_of\_samples$  do
9     for  $j \leftarrow 1, number\_of\_beans$  do
10      if  $sample[i] \leq beans[j]$  then
11         $dCDF[j] += 1$ 
12      end if
13    end for
14  end for
15  for  $i \leftarrow 1, number\_of\_beans$  do
16     $normalized\_dCDF[i] = dCDF[k] / number\_of\_samples$ 
17  end for
18 // Estimation phase:
19  for  $i \leftarrow 1, number\_of\_distribution\_models$  do
20    Fit the  $model[i]$  to  $normalized\_dCDF$ 
21    if fitting converges then
22      if parameters are in the range then
23        Add the model to results
24      end if
25    end if
26  end for
27  for  $model \leftarrow 1, number\_of\_fitted\_models$  do
28    Find the model with lowest AIC, BIC
29  end for
30 Output: the best model

```

Fig. 2. Flowchart of the steps in the application of NR in recognizing statistical models.

In telecommunication systems, performances should be as close to real time as possible, and care must be taken not to introduce any significant delays. Bearing that in mind, the dCDF of the received signal should be calculated from a reasonably small number of points (N_s), but taking into account that the shorter signal length does not cause reduced measurement accuracy. In this paper, we decided to use a sample size $N_s = 1000$, as this was found to be sufficient for a reliable estimation of the probability distribution parameters [26]. Another challenge is to determine the appropriate number of bins for the dCDF. An insufficient number of bins can make distributions sacrifice too much information, and excessive bin numbers might distort the curve to overfit data. In this paper, we used $N_b = 50$ beans in the experiments.

For the recognition of signal distributions and the distribution parameters, we used the methods of NR analysis. In our case, the input data points are x and y values of the signal's dCDF, and mathematical models (equations) of the most frequent Cumulative Distribution Functions with their parameters (i.e. Ω , α , K , m from the equations above) as variables. At the output, algorithms present the appropriate models and estimated values of their parameters along with information criteria for model selection. The process that calculates the best fit of the

dCDF of the test data to the pre-defined probability distribution models consists of several steps: (1) setting the initial values of the parameters to be recognized, and their possible ranges, (2) fitting the model, (3) checking the convergence and the parameter value constraints, and (4) choosing the best model.

There are many statistical software packages on the market that support nonlinear model fitting. In this paper, we used the programming language R (version 4.1.1) and its nlsLM framework [27]. The Levenberg–Marquardt algorithm [28] from the nlsLM framework combines the Gauss–Newton and the Gradient Descent minimization algorithms to solve nonlinear least squares problems. Using this algorithm, we fitted the parameterized mathematical models of probability distributions to the normalized dCDF data points and found the optimal parameters that minimize the residual sum of squares.

We used two model selection criteria for finding the best fit: Akaike's Information Criteria (AIC) and Bayesian Information Criteria (BIC) [29]. AIC and BIC are among the best-known statistical model selection criteria with a wide range of uses. These criteria complement each other: AIC is used for predicting future data as a criterion of model adequacy, while BIC is used for identifying models with the highest probabilities of being true models for the data [30].

In order to obtain experimental results, the authors wrote an R script that implements the steps of the methodology outlined above. This script receives a signal as input, processes it and calculates the dCDF, then fits the distribution models and checks whether the parameters of the successfully fitted models are within the reference values reported in literature [14]. The advantage of this approach is pipeline processing, i.e. the input signal can be processed in real time up to the desired number of measurements, while the probability distribution models can be evaluated. The system rejects those fitted models whose parameters are outside the expected ranges, and then selects the best among the remaining models. The model with the lowest value of the AIC and BIC parameters is selected. The pseudocode algorithm of the steps taken in preparation and implementation of this method is shown in Fig. 2.

4. RESULTS AND DISCUSSION

For this analysis, we used MATLAB to generate 100 signals with N_s data points for each of the 384 combinations of parameters, and thus simulate input signal diversity. The model fitting was applied to each of the signals and the best possible fit was identified. In the following tables, the results of the experiments are presented in a way that row and column headers show the

Table 1. Gamma distribution fitting results

Gamma	$c = 1$	$c = 1.5$	$c = 2$	$c = 2.5$	$c = 3$
$1.0 \leq \Omega \leq 1.3$	100	82.25	92.25	93.75	97.25
$1.4 \leq \Omega \leq 1.7$	100	78.75	89	92.75	96.75
$1.8 \leq \Omega \leq 2.1$	100	79.75	88.75	93	98
$2.2 \leq \Omega \leq 2.5$	100	79.5	88.5	93.75	99.25
AVERAGE	100	80.06	89.63	93.31	97.81

Table 2. Rayleigh distribution fitting results

Rayleigh	Rayleigh	Rician	Nakagami	Weibull	TOTAL
$1.0 \leq \Omega \leq 1.3$	34.25	19	19.25	27.5	100
$1.4 \leq \Omega \leq 1.7$	31	19.25	18.5	31.25	100
$1.8 \leq \Omega \leq 2.1$	31.5	20	17	31.5	100
$2.2 \leq \Omega \leq 2.5$	33.5	19.75	16.5	30.25	100
AVERAGE	32.56	19.5	17.81	30.13	100

Table 3. Rician distribution fitting results

Rician	$K = 0$	$K = 1$	$K = 2$	$K = 3$	$K = 4$	$K = 5$
$1.0 \leq \Omega \leq 1.3$	100	73.75	78.25	73.75	73	89.5
$1.4 \leq \Omega \leq 1.7$	100	73	75.25	68.25	64.5	92.5
$1.8 \leq \Omega \leq 2.1$	100	73	74.75	67.75	70.75	91.25
$2.2 \leq \Omega \leq 2.5$	100	74.25	72.75	71.25	68.5	87.75
AVERAGE	100	73.5	75.25	70.25	69.19	90.25

selected parameter values of the generated signals, while the table cell values show the percentage of correct identifications. The axes labels in further figures (x and y) represent r and the cumulative of $f_R(r)$ from the equations 2–6.

4.1. Gamma distribution

Table 1 presents the results of fitting the Gamma distribution signals with different values of the shape parameter c . The results show that the applied algorithm gives a high percentage of correct recognition of the Gamma distribution, and, furthermore, that the scale parameter Ω has no evident effect on the estimation results.

When the shape parameter of the Gamma (parameter c) and Weibull (parameter α) distributions is equal to one, we obtain a special case of these two distributions – they become exponential distributions [25]. This means that the curves of these two distributions have the same shape. As a result, there is an approximately equal probability that the algorithm will ‘recognize’ the signal as a Gamma or as a Weibull distribution, and the summarized estimation results give 100% successful recognition.

4.2. Rayleigh distribution

The Rayleigh distribution is a special case of several distributions:

- For parameter $K = 0$, equation (4) is reduced to equation (3), i.e. a special case when the Rician distribution becomes the Rayleigh distribution [22].
- For parameter $m = 1$, equation (5) is reduced to equation (3), i.e. a special case when the Nakagami- m distribution becomes the Rayleigh distribution [21].
- For parameter $\alpha = 2$, equation (6) is reduced to equation (3), i.e. a special case when the Weibull distribution becomes the Rayleigh distribution [24].

Due to the abovementioned relationships among probability distributions, the algorithm randomly recognizes the distributions of signals as one of the distributions in the set, but in total the recognition results are 100%.

For illustrative purposes, Table 2 displays the recognition results for signals whose data are generated with the Rayleigh distribution.

4.3. Rician distribution

Table 3 presents the results of fitting the Rician distribution signals with different values of the K factor. The scale parameter Ω has no evident effect on the estimation results.

As stated above, $K = 0$ is a special case when the Rician distribution becomes the Rayleigh distribution, and both the Nakagami- m distribution for $m = 1$ and the

Weibull distribution for $\alpha = 2$ represent a special case of becoming the Rayleigh distribution. The recognition results of 100% can be seen in the corresponding column of Table 3.

4.4. Nakagami-m distribution

In Table 4, the recognition results of signals generated with the Nakagami-m distribution are presented. A high percentage (~90%) of correct recognition of the Nakagami-m distribution is achieved, except for the results with the parameter $m = 1$, where the 100% recognition is achieved. As before, the parameter Ω shows no influence on the recognition results.

When the parameter m approaches 1, the Nakagami-m distribution becomes Rayleigh, while both Rician ($K = 0$) and Weibull ($\alpha = 2$) have an overlapping special case of becoming the Rayleigh distribution. The recognition results of 100% can be seen in the corresponding column of Table 4.

4.5. Weibull distribution

In Table 5, the results of fitting the Weibull distribution with different values of the parameter α are presented. There is a strong dependence of recognition results on the value of the parameter α , while the parameter Ω has no influence. As the parameter α value increases, the accuracy percentage of the Weibull distribution identification decreases.

There are two columns in Table 5 with the results of 100% of correctly identified signals. As stated before, this is due to two special cases: when α approaches 1, Weibull becomes the exponential distribution, and when α approaches 2, Weibull becomes the Rayleigh distribution.

4.6. Illustrative curve fitting plots

Below we present figures showing some illustrative cases of model fitting. While we do provide the AIC and BIC values in these figures, it should be noted that the individual AIC and BIC values should not be interpreted in absolute terms, but rather as differences in values between them [29]. These criteria have no particular value that can be regarded as a threshold, and because this is affected by arbitrary scaling constants and sample sizes, they have a wide range of possible values ([29] reports an indecisive range from -600 to 340 000). In cases where these values are relatively large compared to the differences between them, these differences may appear to be trivial. However, only these differences between values can be interpreted as the proof of a correct model fit, since they are not affected by the scaling parameters.

Figure 3 displays the results of fitting the Rician distribution signal with the parameters $\Omega = 1$ and $K = 5$. Two cases are presented: selecting the best fit considering the expected parameter range and selecting the best fit without considering the expected range. The system tries to fit all the models and finds that only the Rician and Nakagami-m distribution parameters are within the expected range;

Table 4. Nakagami-m distribution fitting results

Nakagami-m	$m = 0.5$	$m = 1$	$m = 2$	$m = 3$	$m = 4$	$m = 5$
$1.0 \leq \Omega \leq 1.3$	94.5	100	91	91	89.75	85.5
$1.4 \leq \Omega \leq 1.7$	94	100	92.25	93	89.25	87.75
$1.8 \leq \Omega \leq 2.1$	92.5	100	90.75	89.5	90.5	88
$2.2 \leq \Omega \leq 2.5$	94.5	100	92.5	94.25	89.25	86
AVERAGE	93.88	100	91.63	91.94	89.69	86.81

Table 5. Weibull distribution fitting results

Weibull	$\alpha = 0.5$	$\alpha = 1$	$\alpha = 1.5$	$\alpha = 2$	$\alpha = 2.5$	$\alpha = 3$
$1.0 \leq \Omega \leq 1/3$	100	100	85.25	100	54	61
$1.4 \leq \Omega \leq 1.7$	99.75	100	83	100	51.5	61.75
$1.8 \leq \Omega \leq 2.1$	100	100	85.75	100	50	60.5
$2.2 \leq \Omega \leq 2.5$	100	100	89.25	100	53.25	58.5
AVERAGE	99.94	100	85.81	100	52.19	60.44

the system checks the AIC and BIC values and successfully identifies the Rician distribution. The estimated parameter values are $\Omega = 0.99$ and $K = 4.71$.

Figure 4 displays the same case of model fitting as Fig. 3 but without the parameter range checking. The

system finds the best fit for the Weibull distribution model despite the fact that the parameter $\alpha = 3.8$ is outside the reference values [14].

In Fig. 5, a representative example of fitting the overlapping distributions is presented; the figure displays the

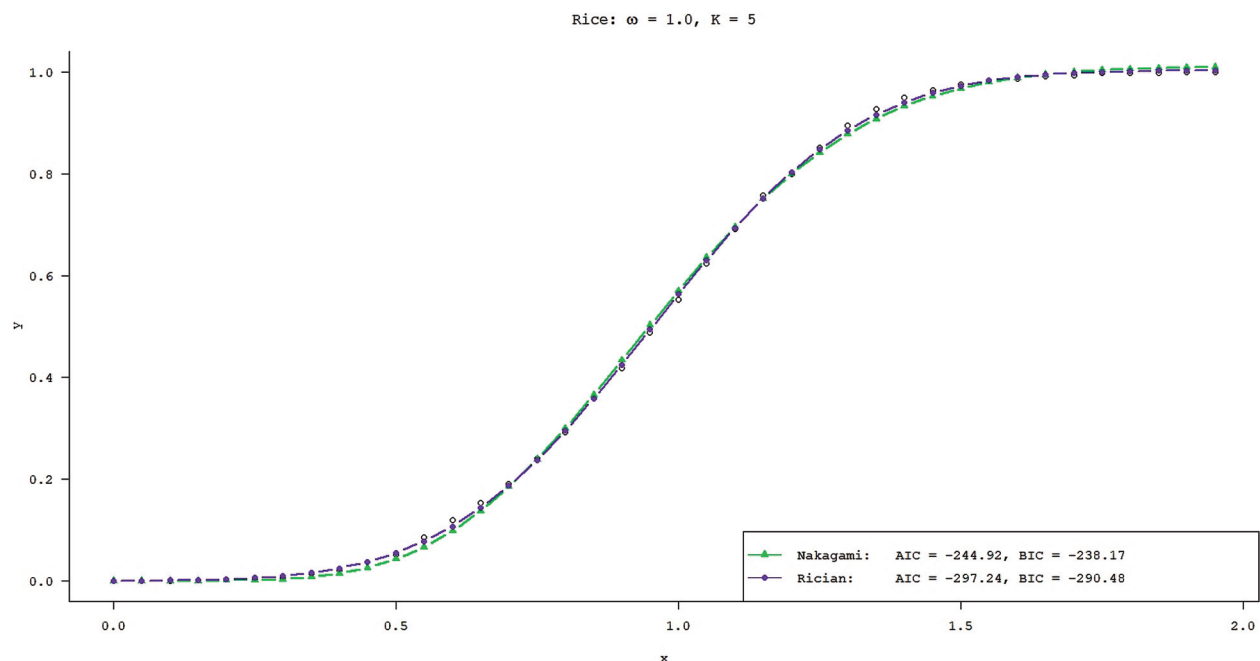


Fig. 3. Limited curve fitting.

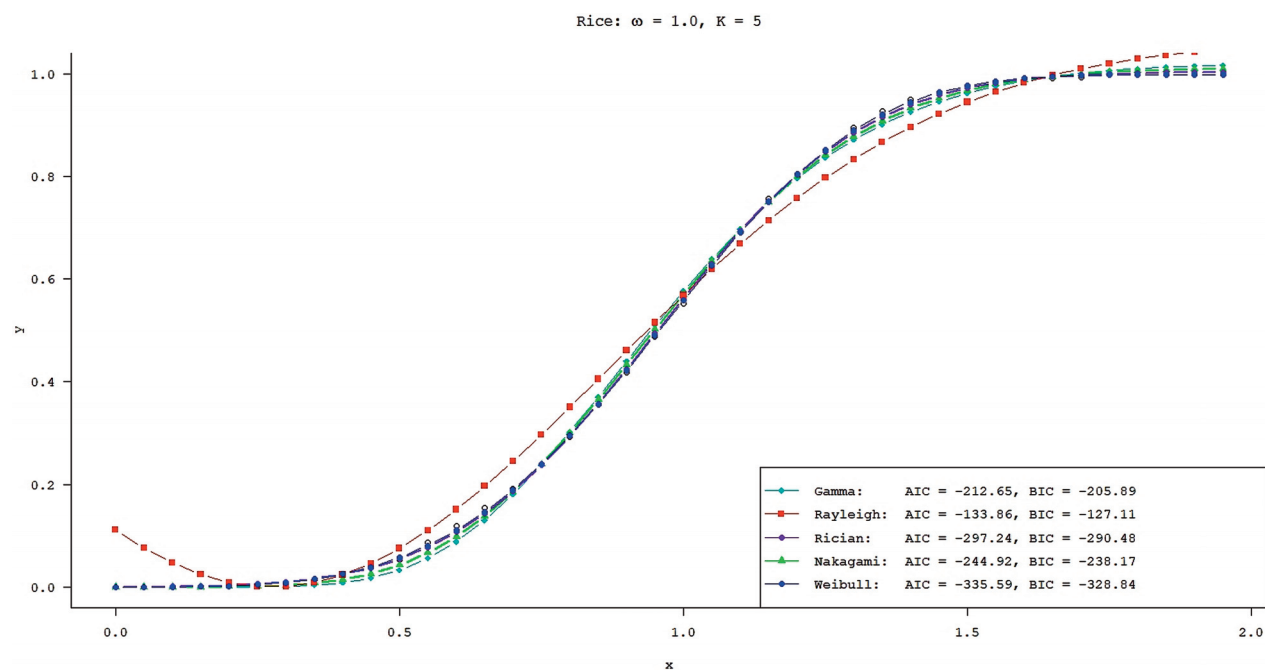


Fig. 4. Unlimited curve fitting.

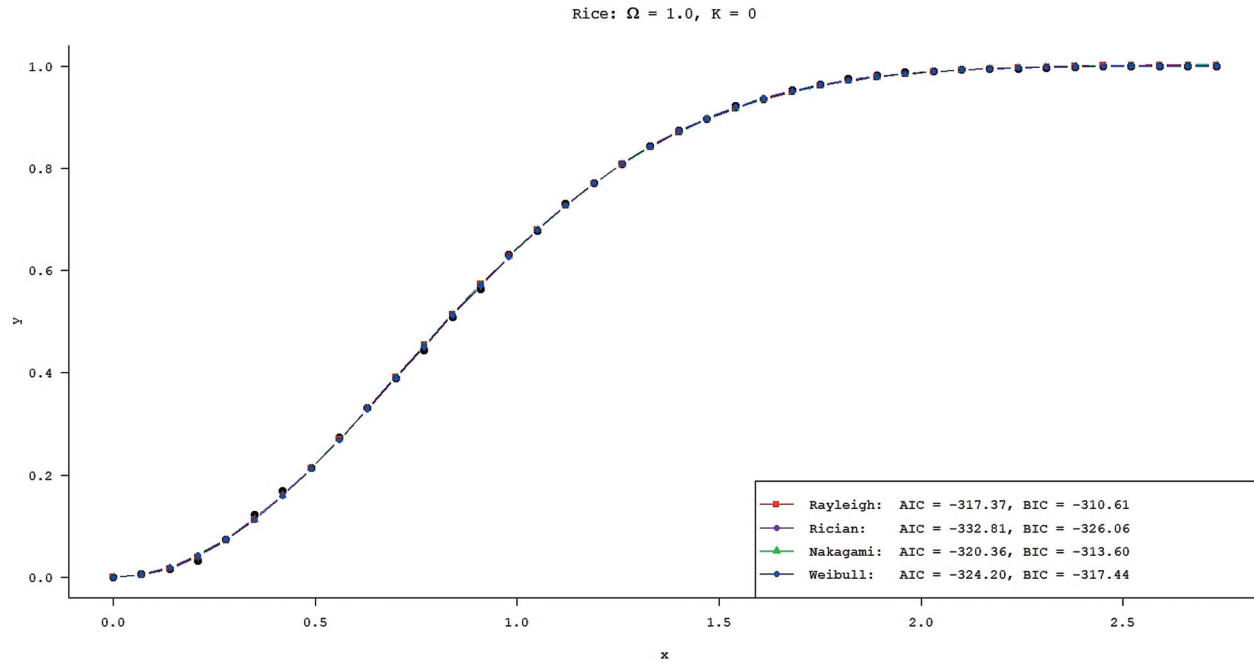


Fig. 5. Fitting the Rician distribution when $K = 0$.

fitting of the Rician distribution signal with the parameters $K = 0$ and $\Omega = 1$. As stated previously, this is the case when the Rician distribution overlaps with the Nakagami-m distribution with the parameter $m = 1$, the Weibull distribution with the parameter $\alpha = 2$, and the Rayleigh distribution. As can be seen in Fig. 3, the AIC and BIC parameter values are close, which is to be expected considering that these distributions overlap.

5. CONCLUSIONS

This paper presents a new approach to using nonlinear regression for calculating the statistical models of wireless channel identification. The given model provides the means for not only recognizing statistical distributions of wireless channels, but also for estimating the parameter values of these distributions. The proposed algorithm is able to recognize the correct distribution without prior knowledge about the input signal, using only predefined probability distribution models. The algorithm is applied to the Gamma, Rayleigh, Rician, Nakagami-m, and Weibull distributions. The results of the executed simulations show a high percentage of successful identifications for all the distributions, even in the special cases, where the statistical model of a wireless channel may be described by any of the several statistical distributions. Furthermore, the results show that the scale parameter Ω of some distributions does not affect the distribution

recognition results, which was to be expected, since the scale parameter is a measure of the spread of a distribution, but has no effect on its skewness. As noted earlier, it is the shape parameter that determines the special cases when these distributions are equivalent or approximate to other distributions.

The obtained results may have practical usage in helping designers of wireless communication systems to design them with optimal parameter values of distribution models, and to obtain the best possible system performance (select the signal with the best performance) in receiving and processing signals from wireless channels. The insights gained from this paper may be of assistance in other fields, where probability distribution models can be applied. Moreover, the fact that this approach does not use prior knowledge about the input signal, it can potentially reduce the design and implementation complexity. Future research could include enhancing the methodology for a better detection of special cases when one distribution transforms to another with a certain combination of parameters, and for recognizing the more complex distribution models that are used in fading channels.

ACKNOWLEDGEMENT

The publication costs of this article were partially covered by the Estonian Academy of Sciences.

REFERENCES

1. Motulsky, H. J. and Ransnas, L. A. Fitting curves to data using nonlinear regression: a practical and nonmathematical review. *FASEB J.*, 1987, **1**(5), 365–374. <https://doi.org/10.1096/fasebj.1.5.3315805>
2. Draper, N. R. and Smith, H. *Applied Regression Analysis*. John Wiley & Sons, 1998.
3. Tsherniak, A., Vazquez, F., Montgomery, P. G., Weir, B. A., Kryukov, G., Cowley, G. S. et al. Defining a cancer dependency map. *Cell*, 2017, **170**(3), 564–576.e16. <https://doi.org/10.1016/j.cell.2017.06.010>
4. Rashid, U., Kumari, N., Signal, N., Taylor, D. and Vandal, A. C. On nonlinear regression for trends in split-belt treadmill training. *Brain Sci.*, 2020, **10**(10), 737. <https://doi.org/10.3390/brainsci10100737>
5. Hahne, J. M., Bießmann, F., Jiang, N., Rehbaum, H., Farina, D., Meinecke, F. C. et al. Linear and nonlinear regression techniques for simultaneous and proportional myoelectric control. *IEEE Trans. Neural Syst. Rehabil. Eng.*, 2014, **22**(2), 269–279. <https://doi.org/10.1109/TNSRE.2014.2305520>
6. Bennink, E., Riordan, A. J., Horsch, A. D., Dankbaar, J. W., Velthuis, B. K. and de Jong, H. W. A fast nonlinear regression method for estimating permeability in CT perfusion imaging. *J. Cereb. Blood Flow Metab.*, 2013, **33**(11), 1743–1751. <https://doi.org/10.1038/jcbfm.2013.122>
7. Tufaner, F. and Demirci, Y. Prediction of biogas production rate from anaerobic hybrid reactor by artificial neural network and nonlinear regressions models. *Clean Technol. Environ. Policy*, 2020, **22**(3), 713–724. <https://doi.org/10.1007/s10098-020-01816-z>
8. Li, W., Shao, L., Wang, W., Li, H., Wang, X., Li, Y. et al. Air quality improvement in response to intensified control strategies in Beijing during 2013–2019. *Sci. Total Environ.*, 2020, **744**, 140776. <https://doi.org/10.1016/j.scitotenv.2020.140776>
9. Tümer, A. E. and Edebalı, S. Prediction of wastewater treatment plant performance using multilinear regression and artificial neural networks. In *Proceedings of the 2015 International Symposium on Innovations in Intelligent Systems and Applications (INISTA), Madrid, Spain, 2–4 September 2015*. IEEE, 1–5. <https://doi.org/10.1109/INISTA.2015.7276742>
10. Wang, J., Li, W., Yang, B., Cheng, X., Tian, Z. and Guo, H. Impact of hydrological factors on the dynamic of COVID-19 epidemic: A multi-region study in China. *Environ. Res.*, 2021, **198**, 110474. <https://doi.org/10.1016/j.envres.2020.110474>
11. Luo, Y., Yan, J. and McClure, S. Distribution of the environmental and socioeconomic risk factors on COVID-19 death rate across continental USA: a spatial nonlinear analysis. *Environ. Sci. Pollut. Res.*, 2021, **28**(6), 6587–6599. <https://doi.org/10.1007/s11356-020-10962-2>
12. Namasudra, S., Dhamodharavadhani, S. and Rathipriya, R. Nonlinear neural network based forecasting model for predicting COVID-19 cases. *Neural Process. Lett.*, 2021. <https://doi.org/10.1007/s11063-021-10495-w>
13. Zhang, L., Shi, Z., Cheng, M.-M., Liu, Y., Bian, J.-W., Zhou, J. T. et al. Nonlinear regression via deep negative correlation learning. *IEEE Trans. Pattern Anal. Mach. Intell.*, 2021, **43**(3), 982–998. <https://doi.org/10.1109/TPAMI.2019.2943860>
14. Panic, S., Stefanovic, M., Anastasov, J. and Spalevic, P. *Fading and Interference Mitigation in Wireless Communications*. CRC Press, Boca Raton, 2015. <https://doi.org/10.1201/b16275>
15. Simon, M. K. and Alouini, M.-S. *Digital Communication Over Fading Channels*. Wiley, 2005.
16. Rice, J. A. Estimation of parameters and fitting of probability distributions. In *Mathematical Statistics and Data Analysis*. Cengage Learning, 2006.
17. Wang, N., Song, X. and Cheng, J. Generalized method of moments estimation of the Nakagami-m fading parameter. *IEEE Trans. Wirel. Commun.*, 2012, **11**(9), 3316–3325. <https://doi.org/10.1109/TWC.2012.071612.111838>
18. Bouhlel, N. and Dziri, A. Maximum likelihood parameter estimation of Nakagami-Gamma shadowed fading channels. *IEEE Commun. Lett.*, 2015, **19**(4), 685–688. <https://doi.org/10.1109/LCOMM.2015.2394293>
19. Alymani, M. *Fading Channel Parameter Estimation Using Deep Learning*. Stevens Institute of Technology, Hoboken, NJ, 2021.
20. Stüber, G. L. *Principles of Mobile Communication*. Springer International Publishing, Cham, 2017. <https://doi.org/10.1007/978-3-319-55615-4>
21. Suraweera, H. A., Louie, R. H. Y., Li, Y., Karagiannidis, G. K. and Vucetic, B. Two hop amplify-and-forward transmission in mixed rayleigh and rician fading channels. *IEEE Commun. Lett.*, 2009, **13**(4), 227–229. <https://doi.org/10.1109/LCOMM.2009.081943>
22. Bernadó, L., Zemen, T., Karedal, J., Paier, A., Thiel, A., Klemp, O. et al. Multi-dimensional K-factor analysis for V2V radio channels in open sub-urban street crossings. In *Proceedings of the 21st Annual IEEE International Symposium on Personal, Indoor and Mobile Radio Communications, Istanbul, Turkey, 26–30 September 2010*. IEEE, 58–63. <https://doi.org/10.1109/PIMRC.2010.5671774>
23. Stefanović, D., Panic, S. and Spalevic, P. Second-order statistics of SC macrodiversity system operating over Gamma shadowed Nakagami-m fading channels. *AEU – Int. J. Electron. Commun.*, 2011, **65**, 413–418. <https://doi.org/10.1016/j.aeue.2010.05.001>
24. Reig, J. Multivariate Nakagami-m distribution with constant correlation model. *AEU – Int. J. Electron. Commun.*, 2009, **63**(1), 46–51. <https://doi.org/10.1016/j.aeue.2007.10.009>
25. Panić, S. R., Stefanović, M., Anastasov, J. and Spalević, P. Modeling of fading channels. In *Fading and Interference Mitigation in Wireless Communications*. CRC Press, 2014.
26. Chen, Y. and Beaulieu, N. C. Estimation of Ricean and Nakagami distribution parameters using noisy samples. In *Proceedings of 2004 IEEE International Conference on Communications, Vol. 1, Paris, France, 20–24 June 2004*. IEEE, 562–566. <https://doi.org/10.1109/ICC.2004.1312552>
27. Elzhov, T. V., Mullen, K. M., Spiess, A.-N. and Bolker, B. minpack.lm: R interface to the Levenberg–Marquardt nonlinear least-squares algorithm found in MINPACK, plus support for bounds, 2022.
28. Gavin, H. P. The Levenberg–Marquardt algorithm for nonlinear least squares curve-fitting problems. *Dep. Civ. Environ. Eng. Duke Univ.*, 2019, **19**.

29. Burnham, K. P. and Anderson, D. R. Multimodel inference: understanding AIC and BIC in model selection. *Sociol. Methods Res.*, 2004, **33**(2), 261–304. <https://doi.org/10.1177/0049124104268644>
30. Kuha, J. AIC and BIC: Comparisons of assumptions and performance. *Sociol. Methods Res.*, 2004, **33**(2), 188–229. <https://doi.org/10.1177/0049124103262065>

Mittelineaarse regressiooni meetod traadita side signaalide levimudeli tuvastamisel

Dragiša Miljković, Siniša Ilić, Dragana Radosavljević ja Stefan Pitulić

Paljudes siderakendustes on oluline tuvastada empiiriliste andmete jaotusseadust võimalikult reaalaaja lähedaselt. Üks spetsiifilisi rakendusi traadita sidesüsteemide puhul on statistiliste mudelite tuvastamine levikeskkonnast tingitud tugi-jaama ja vastuvõtjate vaheliste signaalide sumbumisel (*fading*), mis on üks kõige olulisemaid probleeme antennide ruumilise eraldatuse määramisel. Käesolevas artiklis kirjeldatakse mittelineaarse regressiooni metoodikat ning rakendamise tulemusi sisendsignaali jaotuse ja selle parameetrite väärtuste tuvastamisel. Lisaks saab pakutud lähenemisviisi kasutada reaalaajas sidesignaali jaotusseaduse määramiseks ilma sisendsignaali kohta eelnevat infot omamata. Levenbergi–Marquardti mittelineaarsel vähimruutude meetodil põhinevat algoritmi testitakse suure hulga Gamma, Rayleigh', Rice'i, Nakagami-m ja Weibulli jaotuste põhiselt genereeritud signaalide abil. Eksperimentaalsed tulemused näitavad, et see lähenemine on täpne signaali statistilise levimudeli tuvastamiseks.